PART
I

Types of Imaging Reporter Genes

1 Fluorescent Reporter Proteins

Robert E. Campbell and Michael W. Davidson

INTRODUCTION

For more than a decade the growing class of fluorescent proteins (FPs) defined as homologues of ***Aequorea victoria*** green FP (avGFP), which are capable of forming an intrinsic chromophore, has almost single-handedly launched and fueled a new era in cell biology. These powerful research tools provide investigators with a means of fusing a genetically encoded optical probe to any one of a practically unlimited variety of protein targets to examine living systems using fluorescence microscopy and related methodology (see Figure 1.1; for recent reviews, see references [1–4]). The diverse array of practical applications for FPs ranges from targeted markers for organelles and other subcellular structures, to protein fusions designed to monitor mobility and dynamics, to reporters of transcriptional regulation (Figure 1.2). FPs have also opened the door to creating highly specific biosensors for live-cell imaging of numerous intracellular phenomena, including pH and ion concentration fluctuations, protein kinase activity, apoptosis, voltage, cyclic nucleotide signaling, and tracing neuronal pathways [5–9]. In addition, by applying selected promoters and targeting signals, FP biosensors can be introduced into an intact organism and directed to specific tissues, cell types, and subcellular compartments to enable monitoring a variety of physiological processes using fluorescence resonance energy transfer (FRET) techniques.

If FPs are the "fuel" for the live-cell imaging revolution, the "engines" are the technical advances in widefield fluorescence and confocal microscopes. Some notable advances include low light level digital charge coupled device (CCD) cameras as well as spinning-disk and swept-field instruments. As of today, avGFP and its color-shifted variants, in conjunction with sophisticated imaging equipment, have demonstrated invaluable service in many thousands of live-cell imaging experiments. One of the most important features of FPs is that they are minimally invasive for living cells, especially compared to many traditional synthetic fluorophores (that are often toxic or photoreactive). The relatively low or nonexistent toxicity of FPs (when expressed at low levels relative to endogenous proteins) permits visualization and recording of time-lapse image sequences for extended periods of time [10, 11]. As we will discuss in this chapter, continued advances in FP engineering technology have enabled the fine-tuning of critical fluorescent imaging parameters, including brightness, spectral profiles, photostability, maturation time, and pH insensitivity, to provide a stream of new and advanced probes for optical microscopy. These structural and functional enhancements have stimulated a wide variety of investigations into protein dynamics and function using FP chimeras imaged at low light intensities for many hours to extract valuable biochemical information.

Today we take the exceptional and revolutionary utility of FPs for granted, and it may be hard for some researchers to imagine research without them. It is therefore somewhat surprising that more than 30 years had to pass between the first scientific report of the isolation of avGFP [12] and its first application as a tool for biological imaging [13]. The first report of fluorescence in the bioluminescent hydrozoan jellyfish species *Aequorea victoria* was recorded more than 60 years ago [14] and a protein extract was independently demonstrated by two investigators to be responsible for this "green" fluorescence in the 1960s and 1970s [12, 15]. It took several more decades to identify the responsible protein, clone the gene encoding the protein, and elucidate the primary amino acid structure [16]. In light of the time span between the original discovery and cloning of avGFP, it is rather remarkable that only 2 years later, an image revealing the fluorescent sensory neurons of the nematode highlighted with the same jellyfish protein was featured on the cover of the journal *Science* [13]. This landmark event unambiguously demonstrated the utility of avGFP as a genetic marker in cells evolutionarily far removed from hydrozoans and ushered in a new

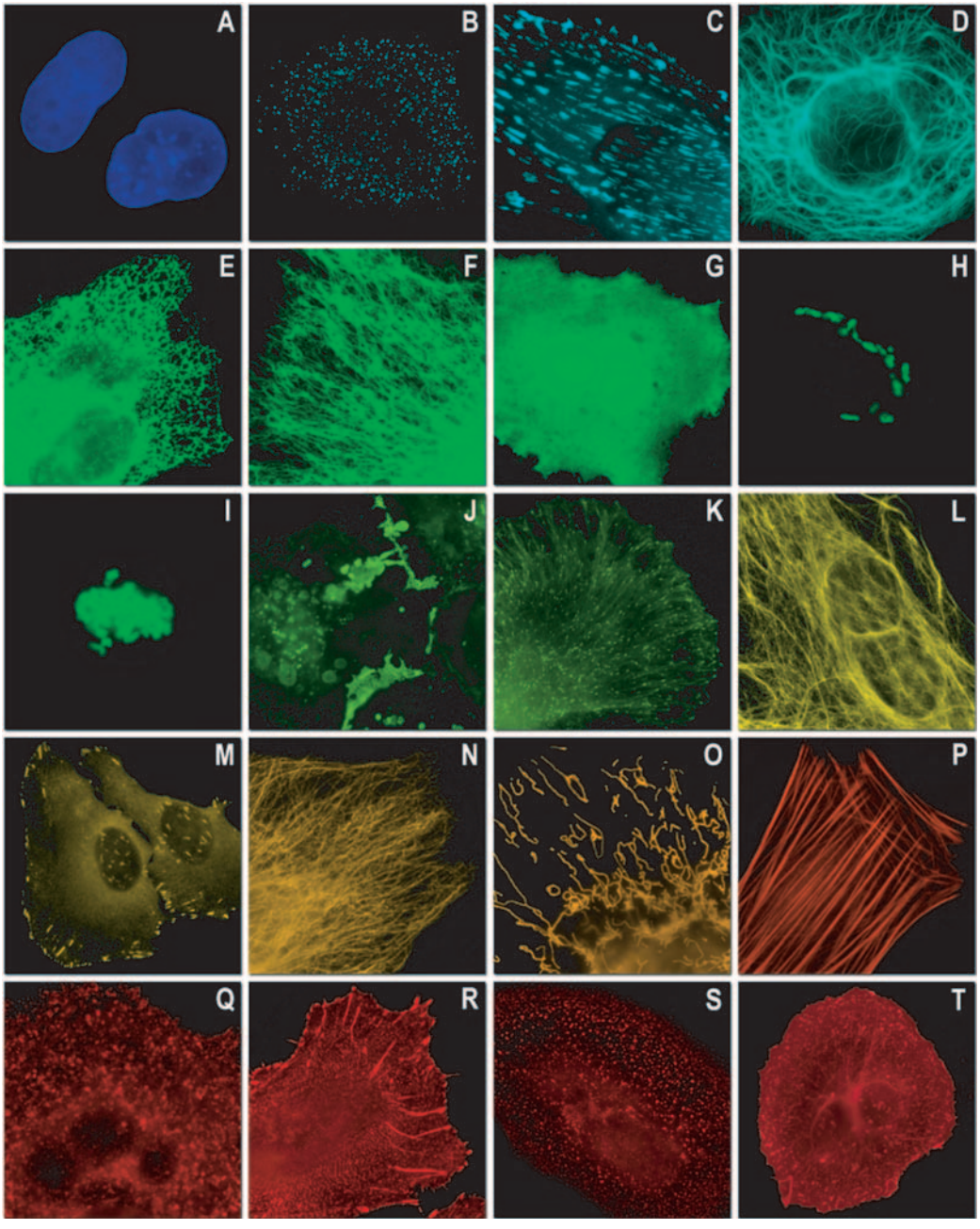

Figure 1.1. Subcellular localization of selected FP fusions (listed in Table 1.1) with targeting proteins imaged in widefield fluorescence. Images are pseudocolored to match the FP emission profile. The FP fusion terminus and number of linker amino acids is indicated after the name of the targeted organelle or fusion protein. The fusion protein and host cell line is given in parentheses (**A**) EBFP2-lamin-B1-N-10 (human lamin B1; nuclear envelope; HeLa); (**B**) ECFP-peroxisomes-C-2 (peroximal targeting signal 1; PTS1; HeLa); (**C**) mCerulean-vinculin-C-23 (human; focal adhesions; Fox Lung); (**D**) mTFP1-keratin-N-17 (human cytokeratin 18; intermediate filaments; HeLa); (**E**) EGFP-endoplasmic reticulum-N-3 (calreticulin signal sequence and KDEL retention sequence; HeLa); (**F**) mEmerald-vimentin-N-7 (human vimentin; intermediate filaments; HeLa); (**G**) mAzami Green-N1 (cloning vector; whole cell fluorescence; HeLa); (**H**) Superfolder avGFP-Golgi-N-7 (N-terminal 81 amino acids of human β-1,4-glactosyltransferase; Golgi complex; HeLa); (**I**) mT-Sapphire-H2B-N-6 (human histone H2B; metaphase; HeLa); (**J**) mVenus-Cx43-N-7 (rat α-1 connexin-43; gap junctions; HeLa); (**K**) YPet-EB3-N-7 (human microtubule-associated protein; RP/EB family; Fox Lung); (**L**) mKusabira Orange-vimentin-N-7 (human; intermediate filaments; Opossum Kidney); (**M**) tdTomato-paxillin-N-22 (chicken; focal adhesions; Fox Lung); (**N**) TagRFP-tubulin-C-6 (human α-tubulin; microtubules; HeLa); (**O**) DsRed2-mitochondria-N-7 (human cytochrome C oxidase subunit VIII; mitochondria; HeLa); (**P**) mStrawberry-actin-C-7 (human β-actin; filamentous actin; Fox Lung); (**Q**) mRFP1-lysosomes-C-20 (rat lysosomal membrane glycoprotein 1; HeLa); (**R**) mCherry-α-actinin-N-19 (human nonmuscle; cytoskeleton; HeLa); (**S**) mKate-clathrin light chain-C-15 (human; clathrin vesicles; HeLa); (**T**) mPlum-farnesyl-C-5 (20-amino acid farnesylation signal from c-Ha-Ras; plasma membrane; HeLa).

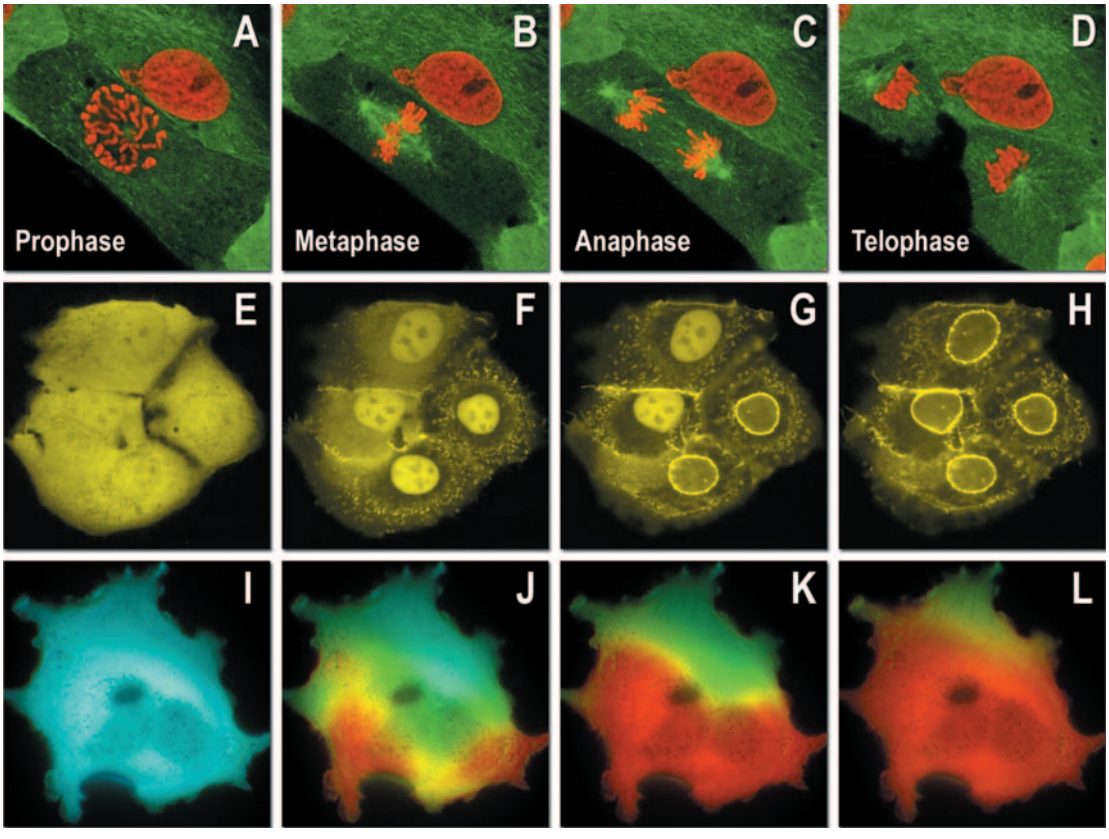

Figure 1.2. Fluorescent protein reporters in action imaged with spinning disk confocal and widefield microscopy. **A–D**: Observing mitosis in dual-labeled normal pig kidney (LLC-PK1 cell line) epithelial cells stably expressing mCherry-H2B-N-6 (histones) and mEmerald-EB3-N-7 (microtubule + end binding protein), (**A**) A cell in prophase (lower) is captured adjacent to a cell in interphase, t = 0; (**B**) The lower cell forms a spindle and enters metaphase. Note the EB3 patterns emanating from the spindle poles and traversing to the plane, t = 20 min; (**C**) During anaphase, the spindle poles translocate to opposite sides of the cell, pulling the condensed chromosomes along, t = 60 min; (**D**) The chromosomes begin to decondense during telophase as the daughter cells recover from cell division (midbody not visible). **E–H**: Spinning disk confocal images selected from a time-lapse series of human cervical adenocarcinoma (HeLa cell line) epithelial cells expressing mKusabira Orange-annexin (A4)-C-12 during ionomycin-induced translocation to the plasma and nuclear membranes, (**E**) A cluster of four cells exhibits expression of the chimera throughout the nucleus and cytoplasm t = 0, ionomycin (10 μM) added; (**F**) Shortly after addition of ionomycin, the annexin chimera begins to translocate to the plasma membrane, clearly revealing the nuclei, t = 3 min; (**G**) The annexin chimera migrates to the membrane in two of the nuclei, time = 5 min; (**H**) The nuclear membranes of all four nuclei display translocated annexin chimera, time = 7 min. (**I–L**) Widefield fluorescence calcium imaging in the cytosol of HeLa cells expressing the circularly permuted cameleon YC3.60; (**I**) Real color image of a single cell, t = 0, histamine (10 μM) added; (**J**) Pseudo-colored ratio image of the HeLa cell as a calcium wave initiates at the two loci on the membrane, t = 10 sec; (**K**) The calcium wave propagates through the cytoplasm, t = 10.5 sec; (**L**) The calcium wave reaches the distant portion of the cell, t = 11.0 sec.

era in biological fluorescence imaging. Through the mid-1990s, a number of genetic variants of the original avGFP nucleotide sequence were developed that featured enhanced green fluorescence (EGFP) [17] and altered fluorescence emission spectral profiles in the blue (BFP) [18, 19], cyan (CFP) [20], and yellow (YFP) [21] regions of the visible spectrum. Perhaps the single most significant advance following the initial cloning and early mutagenesis efforts on wild-type avGFP was the discovery of cyan, green, yellow, orange, and red-fluorescing avGFP homologues in nonbioluminescent reef corals and sea anemones [22]. This discovery not only provided a source of new FPs with new emission colors but also demonstrated that this protein motif can potentially occur in a wide range of classes and species.

FPs have now been discovered in organisms ranging from marine invertebrates to crustaceans and probably exist in many other species [23–26]. In fact, a protein known as nidogen [27], found tucked away in basement membrane of all mammals, has been characterized to have a domain consisting of an 11-stranded β-barrel remarkably similar to the three-dimensional structure of avGFP, despite having only 10% sequence homology.

In nidogen, the amino acid triplet Ile-Gly-Gly (IGG) replaces the chromophore-forming residues Ser-Tyr-Gly (SYG) found in avGFP. In addition, several other residues critical for the generation of a functional chromophore in FPs have been replaced in nidogen by residues that eliminate the possibility of fluorescence. Nevertheless, the β-barrel structure appears to have been evolutionarily conserved for a variety of purposes other than fluorescence, and nature may surprise us again with new sources of chromoproteins and FPs in species previously not considered.

In this chapter, we discuss the basic properties of FPs, including brightness, photostability, color class, oligomerization, folding, and maturation efficiency, and then compare them among themselves and to alternative technologies. In addition, we discuss recent advances in protein engineering strategies as well as improvements to the FP color palette and the development of the current armament of photoactivatable FPs. Finally, we provide suggestions for the best FP choices in single- and multicolor imaging and potential avenues for obtaining the genes encoding these proteins.

COMPARING FLUORESCENT PROTEINS WITH ALTERNATIVE FLUOROPHORES

The single most important advantage of FPs over traditional organic fluorophores and the newer semiconductor quantum dot probes is their widespread compatibility with tissues and intact organisms. In the crowded environment of the cell interior there are thousands of proteins, each with a unique shape, function, and concentration. From the perspective of the cell, expression of the gene encoding an FP (or FP chimera) adds one more relatively benign protein (a perfectly disguised spy!) into this crowded environment. In contrast, a synthetic fluorophore or quantum dot is an unfamiliar and conspicuous entity inside the cell or organism. For example, many synthetic fluorophores are hydrophobic and may bind to exposed hydrophobic patches on other proteins or intercalate into DNA. Furthermore, an FP is created inside the cell from transcription and translation of a gene artificially introduced into the cell's genome. In contrast, synthetic fluorophores and quantum dots are made outside the cell (probably on the lab bench of a chemist) and must breach the cell membrane to reach the cytoplasm, possibly to the detriment of the cell or organism. Other important advantages of FPs include their ability to specifically target fluorescent probes in subcellular compartments and the extremely low or absent levels of phototoxicity. Among the disadvantages of fluorescent proteins are artifacts introduced by delivery of the exogenous nucleic acid, often manifested in high levels of autofluorescence produced by transfection reagents. Overexpression of fluorescent proteins is also a concern but can be offset by careful selection of clones that stably express the fusion products, at appropriate levels.

The advantages of FPs mentioned previously render them the clear and obvious technology of choice for the study of intracellular protein localization and dynamics in living cells or organisms. Simply put, the fact that FPs are *proteins* and are thus *genetically encoded* is an overwhelming advantage relative to all other fluorescent technologies. However, secondary considerations may or may not impact the choice of technology for certain applications, and these will be addressed in the following paragraphs. A number of reviews comparing synthetic dyes, quantum dots, and FP technology have been published in recent years [28–31]. The following sections, rather than repeating the relative merits of each approach, will focus only on some of the most important issues viewed from an FP-centric perspective.

Brightness

The brightness of a fluorophore is proportional to the product of the fluorescence quantum yield (QY) and the extinction coefficient (EC). The EC (units of M^{-1} cm^{-1}) describes how effective a molecule is at absorbing light, whereas the QY (a ratio with no units) is the fraction of the absorbed photons subsequently reemitted as fluorescence. By definition, QY values must lie somewhere between 0 (no fluorescence) and 1 (every absorbed photon is emitted as fluorescence). It is not particularly informative to consider either EC or QY in isolation because the actual fluorescent brightness is proportional to the product of these two values. To put some perspective on relative fluorescent brightness, we will arbitrarily pick two fluorophores useful in live- and fixed-cell imaging, one of which is bright and one of which is relatively dim. The bright fluorophore is sulforhodamine 101 (the sulfonyl chloride form of which is known as Texas Red), which has a fluorescent brightness of 125 mM^{-1} cm^{-1} (i.e., 139,000 M^{-1} cm^{-1} * 0.9) [32]. Note that the units for brightness are arbitrarily provided here as mM^{-1} cm^{-1} (as opposed to M^{-1} cm^{-1} for EC). The relatively dim fluorophore is the cell tracker dye Lucifer yellow CH, which has a fluorescent brightness of 5 mM^{-1} cm^{-1} (24,200 M^{-1} cm^{-1} * 0.21) [32]. Nominally, this brightness range of 5 to 125 mM^{-1} cm^{-1} is an intuitive and convenient yardstick by which to compare different fluorophores. Due to their high ECs and exceptional QYs [33], quantum dots produce brightness values that typically fall into the range of 100–1000 mM^{-1} cm^{-1}, depending on excitation wavelength.

In a head-to-head comparison of the brightness of fluorescein and EGFP, two fluorophores with similar excitation and emission wavelength profiles, fluorescein comes out the winner. The brightness of fluorescein (69 mM^{-1} cm^{-1}) is about double that of EGFP (34 mM^{-1} cm^{-1}) [3]. This single comparison nicely

represents a general trend in comparison of the brightness of FPs and synthetic dyes; FPs are generally dimmer than the highest performance synthetic dyes of similar color. The brightness of FPs spans a broad range with some commercially available proteins, such as mPlum [34] and DsRed-monomer from Clontech (Mountain View, CA), falling near or below the low end of the brightness range provided previously (Table 1.1). At the other extreme, the brightest FPs currently available are YPet at 80 mM^{-1} cm^{-1} [35] and tdTomato at 95 mM^{-1} cm^{-1} [36]. In general, the brightest FPs occur in the green, yellow, and orange color classes, whereas FPs emitting in the blue, cyan, and red spectral regions are generally dimmer. Based on the fact that a number of FPs have ECs approaching 100,000 M^{-1} cm^{-1} and the best have QYs approaching 0.8 [3], it is not unreasonable to expect that it should eventually be possible to engineer an FP color palette where each protein has a brightness of at least 80 mM^{-1} cm^{-1}!

Quantitative assessment of EC and QY for an FP is relatively tedious and requires a highly purified and correctly folded protein with, ideally, greater than 95% of the molecules having an active fluorescent chromophore [37]. In addition, for EC determination the total protein concentration must be accurately determined and the measurements of absorption and fluorescence emission performed in reliable, calibrated instrumentation. QY assessment requires the comparison of emission spectra between the FP and an appropriate reference standard having a similar wavelength profile. Investigators should be highly skeptical of purely qualitative FP brightness evaluations (often made by commercial distributors) that lack quantitative information pertaining to the extinction coefficient and quantum yield. It is difficult, if not impossible, to accurately perform brightness comparisons between FPs without knowledge of these critical parameters. Further complicating matters is the fact that even if EC and QY are highly favorable, experimental brightness observed for the FP gene expressed in living cell is intrinsically dependent on the folding and maturation efficiency of the FP (discussed in the following) [37, 38].

Independent of considerations of the intrinsic brightness displayed by a particular FP, the configuration of the imaging equipment is equally and critically important to achieve high signal strength in an imaging experiment. The laser system or arc-discharge lamp coupled to fluorescence filters used to excite the chromophore should strongly overlap the chromophore absorption profile, and the emission filters must have the widest possible bandpass region coinciding with the emission spectrum. In addition, the camera system must be capable of recording images with high quantum efficiency in the fluorescence emission region of interest [39], and the optical system of the microscope should have high throughput in the wavelength regions necessary for producing excitation and gathering emission. Even with research-level instrumentation, it is often difficult to achieve the maximum potential FP brightness levels in each spectral class unless the fluorescence filter sets are optimized for imaging the proteins. Many multiuser core imaging facilities have limited inventories of filter sets typically designed for traditional synthetic fluorophores rather than FPs. For example, the standard DAPI (4', 6-diamidino-2-phenylindole; ultraviolet excitation), FITC (fluorescein isothiocyanate; cyan–blue excitation), TRITC (tetramethylrhodamine isothiocyanate; green excitation), and Texas Red (yellow excitation) fluorescence filter combinations, often marketed by default with widefield arc-discharge microscopes, are not suitable for many FPs and are less than optimal for others.

Photostability

A commonly cited limitation of FPs relative to other fluorophore technologies is their propensity to photobleach during observation. In other words, illumination of an FP causes it to self-destruct through a series of poorly understood and likely complex mechanisms. Two probable mechanisms for photobleaching of FPs are reaction with a reactive oxygen species (ROS; i.e., singlet oxygen generated by the FP chromophore itself) and photoinduced isomerization [40]. Synthetic dyes are, of course, also susceptible to photobleaching by related mechanisms. One might expect that due to the protective protein shell that holds the FP chromophore rigid and planar and protects it from the bulk environment [41, 42], FPs should be significantly more photostable than a fluorescent dye. Generally speaking, this is not true, and for the FPs considered "best in class," the average photostability is on par with that of the widely used synthetic dye, fluorescein [3]. The most photostable of all currently available monomeric FPs is mEGFP, which is ~33-fold more photostable than fluorescein. The fluorescence of fluorescent nanoparticles (or quantum dots) does not rely on the conjugated systems of double bonds that are the "Achilles heel" of FPs and synthetic dyes with respect to photobleaching. For this reason, nanoparticles have greatly improved photostability over even the best FPs and synthetic dyes [30].

Although there is a high degree of uncorrelated variability between FPs in terms of photostability, most variants listed in Table 1.1 are useful for short-term imaging (from 1 to 25 captures), while several of the more photostable proteins can be employed in time-lapse sequences that span periods of 24 h or longer (in which hundreds to thousands of images are gathered). The long-term stability of any particular protein, however, must be investigated for every illumination scenario (widefield, confocal, multiphoton, swept-field, etc.) because nonlinear differences in photostability are often observed with the

Table 1.1. A compilation of properties of the most useful FP variants. Along with the common name and/or acronym for each FP, the peak excitation (Ex) and emission (Em) wavelengths, molar extinction coefficient (EC), quantum yield (QY), relative brightness, and physiologically relevant quaternary structure are listed (*signifies a weak dimer). The computed brightness values were derived from the product of the molar extinction coefficient and quantum yield, divided by the value for EGFP. This listing was created from scientific and commercial literature resources and is not intended to be comprehensive, but instead represents FP derivatives that have received considerable attention in the literature and may prove valuable in research efforts. The excitation and emission peak values listed may vary in published reports due to the broad spectral profiles. In actual fluorescence microscopy investigations, the experimental brightness of a particular FP may differ (in relative terms) from the brightness provided in this table. Among the many potential reasons for these differences are wavelength-dependent differences in the transmission or reflectance of microscope optics and the efficiency of the camera. Furthermore, the extent of FP folding and maturation will depend on both the particular variant being used as well as the particular characteristics and localization of the fusion partner

Protein (Acronym)	Ex (nm)	Em (nm)	EC × 10^{-3} M^{-1} cm^{-1}	QY	Quaternary Structure	Relative Brightness (% of EGFP)	Reference
Blue Fluorescent Proteins							
Azurite	384	450	26.2	0.55	Monomer*	43	[91]
EBFP2	383	448	32.0	0.56	Monomer*	53	[57]
mTagBFP	399	456	52.0	0.63	Monomer	98	[100]
Cyan Fluorescent Proteins							
ECFP	439	476	32.5	0.40	Monomer*	39	[185]
TagCFP	458	480	37.0	0.57	Monomer	63	Evrogen
mCerulean	433	475	43.0	0.62	Monomer*	79	[88]
CyPet	435	477	35.0	0.51	Monomer*	53	[35]
AmCyan	458	489	44.0	0.24	Tetramer	31	[22]
Midoriishi Cyan	472	495	27.3	0.90	Dimer	73	[73]
mTFP1	462	492	64	0.85	Monomer	162	[77]
Green Fluorescent Proteins							
EGFP	488	507	56.0	0.60	Monomer*	100	[17]
Emerald	487	509	57.5	0.68	Monomer*	116	[97]
Azami Green	492	505	55.0	0.74	Monomer	121	[72]
mWasabi	493	509	70.0	0.80	Monomer	167	[107]
ZsGreen	493	505	43.0	0.91	Tetramer	117	[22]
TagGFP	482	505	58.2	0.59	Monomer	102	Evrogen
Superfolder avGFP	485	510	83.3	0.65	Monomer*	160	[55]
T-Sapphire	399	511	44.0	0.60	Monomer*	79	[44]
Yellow Fluorescent Proteins							
EYFP	514	527	83.4	0.61	Monomer*	151	[186]
Topaz	514	527	94.5	0.60	Monomer*	169	[60]
Venus	515	528	92.2	0.57	Monomer*	156	[56]
Citrine	516	529	77.0	0.76	Monomer	174	[92]
YPet	517	530	104	0.77	Monomer*	238	[35]
ZsYellow	529	539	20.2	0.42	Tetramer	25	[22]
TagYFP	508	524	64.0	0.60	Monomer	118	Evrogen
mAmetrine	406	526	45.0	0.58	Monomer	78	[187]
Orange Fluorescent Proteins							
Kusabira Orange	548	559	51.6	0.60	Monomer	92	[73]
Kusabira Orange2	551	565	63.8	0.62	Monomer	118	[114]
mOrange	548	562	71.0	0.69	Monomer	146	[36]
mOrange2	549	565	58.0	0.60	Monomer	104	[115]
dTomato	554	581	69.0	0.69	Dimer	142	[36]
dTomato-Tandem	554	581	138	0.69	Pseudo Monomer	283	[36]
DsRed	558	583	75.0	0.79	Tetramer	176	[22]
DsRed-Express (T1)	555	584	38.0	0.51	Tetramer	58	[188]
DsRed-Monomer	556	586	35.0	0.10	Monomer	10	Clontech
TagRFP	555	584	100.0	0.48	Monomer	142	[118]
TagRFP-T	555	584	81.0	0.41	Monomer	99	[115]
Red Fluorescent Proteins							
mRuby	558	605	112.0	0.35	Monomer	117	[126]
mApple	568	592	75.0	0.49	Monomer	109	[115]
mStrawberry	574	596	90.0	0.29	Monomer	78	[36]
AsRed2	576	592	56.2	0.05	Tetramer	8	[22]
mRFP1	584	607	50.0	0.25	Monomer	37	[64]
JRed	584	610	44.0	0.20	Dimer	26	[93]
mCherry	587	610	72.0	0.22	Monomer	47	[36]
HcRed1	588	618	20.0	0.015	Dimer	1	[123]
mRaspberry	598	625	86.0	0.15	Monomer	38	[34]
mKate	588	635	45.0	0.33	Monomer	44	[128]
HcRed-Tandem	590	637	160	0.04	Pseudo Monomer	19	[78]
mPlum	590	649	41.0	0.10	Monomer	12	[34]

same protein when illumination is produced by an arc-discharge lamp versus a laser system. The molecular basis of nonlinear differences in photobleaching of FPs versus light intensity and wavelength is largely an open question that we hope will be addressed in the future. In terms of photostability, the selection of a suitable FP is dictated by numerous parameters, including the illumination conditions, the expression system, and the effectiveness of the imaging setup.

Color Class

What does "color" mean in the context of fluorescence? It could, reasonably, refer to the perceived color of a solution of the fluorophore when viewed in white light. The term could also, reasonably, refer to the perceived color of the solution when illuminated with monochromatic light of a wavelength that corresponds to the absorbance maxima. In practice, any attempt to define fluorescence color by virtue of how it is perceived by eye leads to complications. A more rigorous and practical approach to defining fluorescence color is to say that two fluorophores have different color if their excitation and/or emission maxima and/or peak shapes are significantly different. Defining "significantly different" is troublesome as it depends on the instrumentation available for measuring the shape and maxima of the emission and excitation peaks. For example, spectral imaging can be used to differentiate two colors that could not be differentiated through the use of bandpass filters.

Regardless of whether one considers synthetic fluorophores, FPs, or quantum dots and assuming all other considerations are the same, how will the researcher choose which color to use? An important consideration with respect to color selection is the greater desirability of red-shifted fluorophores [43]. It is generally accepted that excitation with violet or blue light is associated with greater cellular phototoxicity than excitation with green, yellow, or longer wavelength light extending through the near infrared (up to ~1000 nm) but not into the true infrared (where heating due to absorption by water would be problematic for cell viability). Fluorescence excitation and emission hues of FPs are confined to a relatively narrow region of the electromagnetic spectrum (essentially the visible wavelengths) due to protein-imposed restrictions on the possible manipulations of the chromophore structure and environment. In contrast, synthetic dyes and nanoparticles with fluorescence emission tuned to wavelengths that cover the visible and near-infrared regions of the spectrum are available. This spectral limitation of FPs is exacerbated by their relatively broad excitation and emission peaks (ranging up to 100 nm) that further restrict the number of colors that can be distinguished with bandpass filters on a widefield microscope. Practically speaking, the bandwidth of the absorption and emission peaks is an important consideration in defining the number of colors that are "spectrally distinct." Roughly speaking, there are currently about ten different emission colors of FPs with short Stoke shifts (defined as the distance in nanometers between the absorption and emission peak wavelengths of a fluorophore) and emission maxima spaced every 20 nm between 450 and 650 nm (Table 1.1). These colors include: blue (~450 nm), cyan (~470 nm), teal (~490 nm), green (~510 nm), yellow (~530 nm), yellow–orange (~550 nm), orange (~570 nm), orange–red (~590 nm), red (~610 nm), and far-red (>630 nm). There are a few additional long Stoke shift FPs such as Sapphire [44] and mKeima [45], which, given the definition of fluorescence color provided previously, should be considered additional color classes. However, due to the relatively broad excitation and emission peaks shared by all FPs, it is only really practical to simultaneously image three (Figure 1.3 [46]) or four distinct colors (such as cyan, yellow, and red or blue, green, orange, and far-red) using a bandpass filter-based microscopy system [3]. However, this tenet does not always hold true as the imaging of six distinct colors (CFP, cyan; mMiCy, teal; EGFP, green; YFP, yellow; dKeima570, orange; and mKeima, red) has been achieved using a single laser line for excitation and spectral unmixing of the emission [45].

Hybrid Approaches

This discussion has established that, relative to synthetic dyes and quantum dots, the physical properties of FPs are less than ideal yet more than adequate. Investigators that simply require a fluorophore with high fluorescent brightness, good photostability, and broad color selection would do better with synthetic dyes or quantum dots. However, as mentioned earlier, such superficial comparisons are a disservice to FPs because the fact that these probes are proteins, and are therefore genetically encodable, is their overwhelming advantage for many biological applications. In recent years there has been significant progress in developing "hybrid" technologies for the protein-specific labeling of recombinant proteins in live cells [47–49]. These approaches typically exploit modified dyes (or quantum dots [50]) for noncovalent binding or covalent attachment to a genetically encoded sequence that can be appended to a recombinant protein of interest. Notable examples of such methods include biarsenical xanthene dye-based labeling of tetracysteine motifs [51] and benzylguanine-dye conjugate-based labeling of O6-alkyguanine-DNA alkyltransferase fusion proteins [52], though a number of additional new systems have been reported [47–49]. Although these techniques hold great promise, none of them has yet achieved the versatility and widespread acceptance of FP-based labeling. A major limitation shared by all hybrid methodologies is the nonspecific labeling of intracellular structures with the exogenously applied dye [53]. In

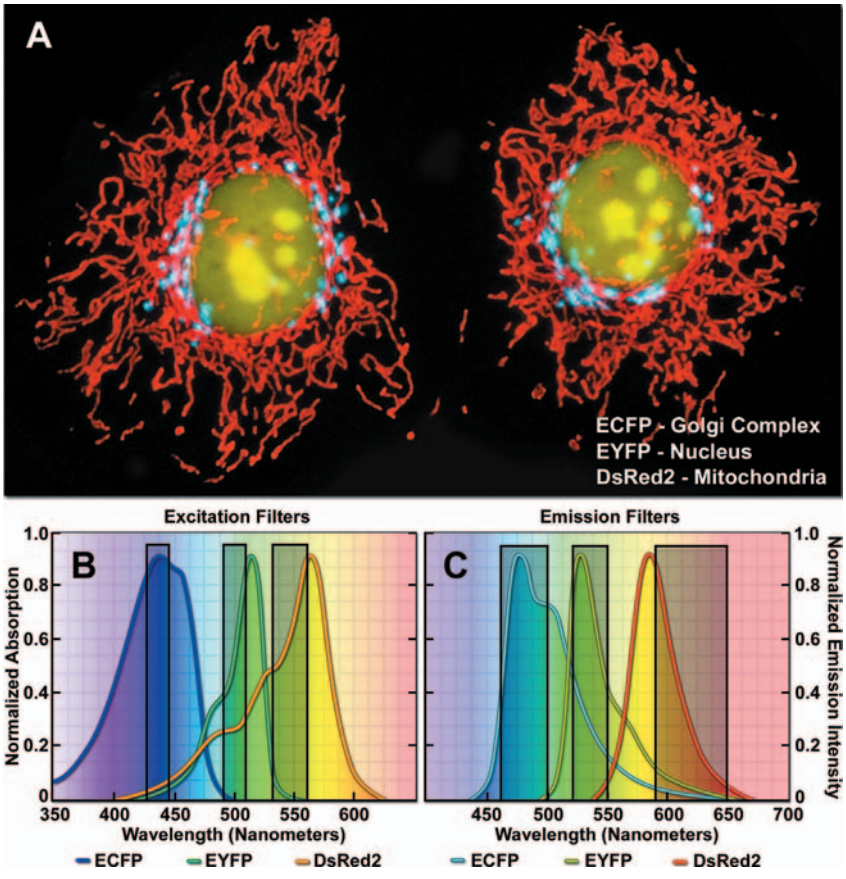

Figure 1.3. Optimized fluorescence filter combinations for multicolor imaging of three FPs spanning the cyan to orange-red wavelength regions; (**A**) Widefield fluorescence image of HeLa cells labeled with ECFP (Golgi complex targeting signal), EYFP (nuclear targeting signal), and DsRed2 (mitochondrial targeting signal); (**B**) Excitation filters optimized for ECFP, EYFP, and DsRed2 FPs having center wavelengths of 436, 500, and 545 nm, respectively. The bandwidth of the ECFP and EYFP excitation filters is 20 nm whereas the bandwidth of the DsRed2 filter is 30 nm; (**C**) Emission filters optimized for the same probes having center wavelengths of 480, 535, and 620 nm with bandwidths of 40, 30, and 60 nm, respectively.

many cases, high levels of nonspecific background staining hampers observation of the targeted structures, and several of the synthetic dyes are sequestered in the mitochondria, lysosomes, and other organelles.

DIRECT COMPARISONS OF FLUORESCENT PROTEINS TO EACH OTHER

For direct comparison of one FP to another, the properties of brightness, photostability, and color remain the three most important criteria. However, there are additional concerns that are direct consequences of the unique experimental designs made possible with FPs. For example, because these probes are proteins, they must undergo efficient transcription, translation, and folding to be functional. Once correctly folded, they then undergo autocatalytic posttranslational chromophore formation, a process informally referred to as "maturation" or "ripening." If the efficiency of any of these steps is compromised, the experimentally observed fluorescence will be diminished or even abolished. Such concerns are not relevant to alternative technologies such as synthetic dyes and quantum dots applied directly to the cells or tissue. In the following sections we list several of the most important criteria that can be used to directly compare FPs and discuss efforts to engineer new variants that are superior by these criteria.

Folding and Maturation Efficiency

Aequorea jellyfish inhabit the cool ocean waters off the coast of Washington and British Columbia. Accordingly, the natural environment of the avGFP protein is one where the temperature hovers around 4–5° C. In contrast, in the unnatural environment (from the FP's perspective) of a transfected cell culture or the cells of a transgenic organism, the avGFP protein will most

often experience much higher temperatures than those in which it was evolved to fold, mature, and function. FPs derived from reef corals and sea anemones generally express well at 37° C without genetic selection, presumably because the native species from which the proteins are obtained have evolved in somewhat warmer habitats [54]. The original transposition of wild-type avGFP from jellyfish to cells grown at 37° C substantially decreased the efficiency with which the protein could fold into its proper three-dimensional (tertiary) structure. Clearly this problem needed to be addressed through protein engineering. Indeed, among the first and most substantial improvements to the avGFP protein were realized by selection of variants with more efficient folding at 37° C. Years of progress in this regard have most recently led to a so-called superfolder avGFP with improved folding kinetics, tolerance to circular permutations, high performance in fusions to poorly folding polypeptides, and resistance to denaturation [55]. One of the more interesting and useful aspects of mutations that improve folding efficiency is that they are often translated to different FP colors where they seem to provide similar improvements. The translation of so-called folding mutations to hue-shifted variants has contributed to the excellent folding properties or high brightness of the Venus YFP variant [56], EBFP2 [57], and the series of "super" cyan and yellow FPs [58, 59], among others [55].

The presence of molecular oxygen is also a critical factor in FP chromophore development during the maturation process. During the formation of chromophores in *Aequorea* protein variants, at least one oxygen molecule is required for an oxidation reaction [60, 61], whereas reef coral proteins that emit in the orange–red spectral regions usually require two molecules [62, 63]. In mammalian cell cultures, FP maturation is rarely hampered by a lack of oxygen, but anoxia could become a limiting factor in other systems.

Oligomerization

All of the FPs discovered to date display at least a limited degree of quaternary structure (self-association of individual protein units), exemplified by the weak tendency of native avGFP and its derivatives to dimerize when immobilized at high concentrations [64, 65], as well as the obligate tetrameric structure characteristic of FPs from reef coral and anemones [66, 67]. Oligomerization can be a significant problem for many applications in cell biology, particularly in cases where the FP is fused to a host protein targeted at a specific subcellular location. Once expressed, the formation of dimers and higher-order oligomers induced by the FP portion of the chimera can produce atypical localization, disrupt normal function, interfere with signaling cascades, or restrict the fusion product to aggregation within a specific organelle or the cytoplasm. This effect is particularly

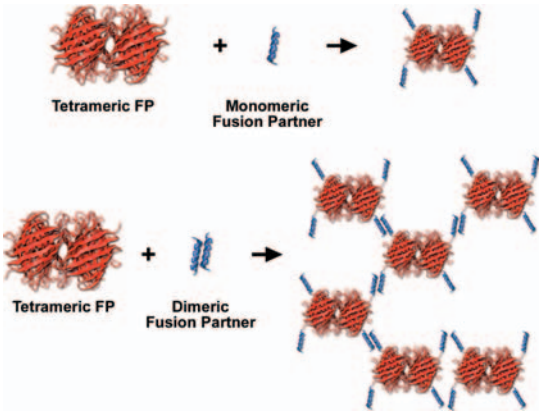

Figure 1.4. Any protein fused to a tetrameric FP will become tetrameric itself.

marked when the FP is fused to partners that participate in natural oligomer formation themselves (see Figure 1.4). Fusion products with proteins that form only weak dimers (i.e., most *Aequorea* variants) may not exhibit aggregation or improper targeting, provided the localized concentration remains low. However, when FPs are targeted to specific cellular compartments, such as the plasma membrane, the localized protein concentration can, in some circumstances, become high enough to permit dimerization.

The basic strategy for overcoming oligomerization artifacts is to modify the FP amino acid sequence to include residues that disrupt intermolecular interactions, a procedure that varies in complexity depending upon the nature and origin of the protein. For many avGFP variants, dimerization can be either significantly reduced or eliminated by replacing the hydrophobic amino acid side chains in the dimer interface with positively charged residues at several key sequence positions [65]. The three most successful mutations, in decreasing order of effectiveness, are A206K, L221K, and F223R, where the nonpolar amino acids alanine, leucine, and phenylalanine are replaced by one of the positively charged hydrophilic amino acids lysine or arginine. In cases where close molecular associations are suspected involving a fusion protein and where quantitative FRET interactions are investigated, it is highly recommended that avGFP variants (i.e., CFP and YFP) be converted into monomers using the A206K point mutation [3, 68].

Creating FP monomers from the tetrameric reef coral and sea anemone proteins is usually far more difficult. Even at exceedingly low concentrations, the original DsRed FP is an obligate tetramer [66] that cannot be dissociated without irreversible denaturation of the polypeptides. In the tetrameric unit, each DsRed protomer interacts with two adjacent neighbors, one through a hydrophobic interface and the other through a hydrophilic interface resulting in a complex assembly